Physics of Fluids

Piston driven converging shock waves in a stiffened gas

Cite as: Phys. Fluids **31**, 086106 (2019); https://doi.org/10.1063/1.5109097
Submitted: 06 May 2019 . Accepted: 06 August 2019 . Published Online: 28 August 2019

Scott D. Ramsey, and Roy S. Baty


View Online

Export Citation

CrossMark

ARTICLES YOU MAY BE INTERESTED IN

Statistics of overpressure fluctuations behind a weak shock wave interacting with turbulence
Physics of Fluids **31**, 085119 (2019); https://doi.org/10.1063/1.5110185

Coherent structures in tornado-like vortices
Physics of Fluids **31**, 085118 (2019); https://doi.org/10.1063/1.5111530

Interaction of cylindrical converging shocks with an equilateral triangular SF_6 cylinder
Physics of Fluids **31**, 086104 (2019); https://doi.org/10.1063/1.5094671

AIP Publishing

© 2019 Author(s).

Physics of Fluids ARTICLE scitation.org/journal/phf

Piston driven converging shock waves in a stiffened gas

Cite as: Phys. Fluids 31, 086106 (2019); doi: 10.1063/1.5109097
Submitted: 6 May 2019 • Accepted: 6 August 2019 •
Published Online: 28 August 2019

View Online Export Citation CrossMark

Scott D. Ramsey[1,a)] and Roy S. Baty[2,b)]

AFFILIATIONS

[1] Applied Physics, Los Alamos National Laboratory, P.O. Box 1663, MS T082, Los Alamos, New Mexico 87545, USA
[2]Applied Physics, Los Alamos National Laboratory, P.O. Box 1663, MS T086, Los Alamos, New Mexico 87545, USA

[a)]ramsey@lanl.gov
[b)]rbaty@lanl.gov

ABSTRACT

The problem of a one-dimensional (1D) cylindrically or spherically symmetric shock wave converging into an inviscid, ideal gas was first investigated by Guderley[Starke kugelige und zylinrische verdichtungsstosse in der nahe des kugelmitterpunktes bzw. Der zylinderachse," Luftfahrtforschung **19**, 302 (1942)]. In the time since, many authors have discussed the practical notion of how Guderley-like flows might be generated. One candidate is a constant velocity, converging "cylindrical or spherical piston," giving rise to a converging shock wave in the spirit of its classical, planar counterpart. A limitation of pre-existing analyses along these lines is the restriction to flows in materials described by an ideal gas equation of state (EOS) constitutive law. This choice is of course necessary for the direct comparison with the classical Guderley solution, which also features an ideal gas EOS. However, the ideal gas EOS is limited in its utility in describing a wide variety of physical phenomena and, in particular, the shock compression of solid materials. This work is thus intended to provide an extension of previous work to a nonideal EOS. The stiff gas EOS is chosen as a logical starting point due to not only its close resemblance to the ideal gas law but also its relevance to the shock compression of various liquid and solid materials. Using this choice of EOS, the solution of a 1D planar piston problem is constructed and subsequently used as the lowest order term in a quasi-self-similar series expansion intended to capture both curvilinear and nonideal EOS effects. The solution associated with this procedure provides correction terms to the 1D planar solution so that the expected accelerating shock trajectory and nontrivially varying state variable profiles can be obtained. This solution is further examined in the limit as the converging shock wave approaches the 1D curvilinear origin. Given the stiff gas EOS is not otherwise expected to admit a Guderley-like solution when coupled to the inviscid Euler equations, this work thus provides the semianalytical limiting behavior of a flow that cannot be otherwise captured using self-similar analysis.

Published under license by AIP Publishing. https://doi.org/10.1063/1.5109097

I. INTRODUCTION

The problem of a one-dimensional (1D) cylindrically or spherically symmetric shock wave converging into an inviscid, perfect gas was first investigated by Guderley[1] in 1942 and independently by Landau and Stanyukovich[2] in 1944. The problem has been frequently revisited in the time since, including by Butler,[3] Lazarus,[4] and Chisnell.[5] The problem's numerous applications can be found in the laser fusion community,[6–9] astrophysical contexts,[10] and verification activities for inviscid compressible flow (Euler) codes.[11]

Using symmetry analysis techniques, it can be shown that the Guderley problem falls within the same family of scale-invariant, self-similar flows as the Noh constant-velocity implosion,[12] and Sedov-von Neumann-Taylor blast wave[13,14] (or "Sedov problem," for simplicity). While at a high level, these solutions are a consequence of scaling groups of the inviscid Euler equations, they are distinguished from one another by different initial conditions (and thus potentially different scaling subgroups). These differences also manifest in the categorization of the problems into Barenblatt's[15,16] first and second-type self-similar solutions: while the Noh and Sedov solutions fall into the first class, the Guderley problem is an archetypal example of the second. The interplay between this notion, initial conditions, and other relevant concepts is discussed at length by Barenblatt,[15,16] Waxman and Shvarts,[17] and Boyd *et al.*[18] A key point of these developments is that while the Noh and Sedov problems are generated by discrete initial events, the Guderley solution

Published under license by AIP Publishing

instead results "from an infinitely weak state, at infinity, infinitely long ago."[19]

This concept notwithstanding, many authors discuss the practical notion of how a Guderley-like flow might be generated. Two obvious candidates are a "cylindrical or spherical shock tube" and a "cylindrical or spherical piston," in each case giving rise to a converging shock wave in the spirit of their classical, planar counterparts (see, for example, the work of Landau and Lifshitz[20] or Zel'dovich and Raizer[21]). The former concept is investigated by Hornung *et al.*[22] and Ramsey and Lilieholm[23] The latter was first investigated by Van Dyke and Guttmann[24] (see also Sachdev[25,26]) and forms the basis of the current work.

An important outcome of Van Dyke and Guttmann's work is the establishment of a quantitative connection between their converging curvilinear piston-driven flow and the Guderley converging shock wave. In particular, Van Dyke and Guttmann demonstrate that their piston-driven converging shock wave asymptotically approaches the corresponding Guderley solution and that there exists a possibility that other piston motions may do likewise.

Despite its utility, one of the limitations of Van Dyke and Guttmann's work is its restriction to flows in materials described by an ideal gas equation of state (EOS) constitutive law. This choice is of course necessary for the direct comparison with the Guderley solution, which also features an ideal gas EOS. However, as has been noted by numerous authors, the ideal gas EOS is limited in its utility to describing flows in noninteracting gases. As a result, some recent studies have been devoted to extending the ideal gas Guderley solution to more broadly applicable classes of EOS.[18,27,28]

The current work is thus intended to provide in parallel the extension of Van Dyke and Guttmann's formalism to a nonideal EOS. The stiff gas EOS as described by Harlow and Amsden[29] and Burnett *et al.*[30] is chosen as a logical starting point due to not only its close resemblance to the ideal gas law but also its relevance to the shock compression of various liquid and solid materials. Moreover, following from the analysis of Boyd *et al.*,[27] the stiff gas EOS is not expected to admit a Guderley-like solution when coupled to the inviscid Euler equations. Therefore, the analysis to follow will provide the semianalytical limiting behavior of a flow that cannot be otherwise captured using self-similar analysis.

In support of the goals described above, the remainder of this article is laid out as follows: more details surrounding the definition of the cylindrical/spherical piston problem are provided in Sec. II, along with the attendant mathematical model. A solution of the converging curvilinear piston problem for a stiff gas (in the spirit of Van Dyke and Guttmann's work[24]) is provided in Sec. III. Conclusions and recommendations for future study appear in Sec. IV.

II. THE PISTON PROBLEM

The principal interest of this work is the problem of a 1D cylindrical or spherical (curvilinear) piston initially located at position $R_{p,0}$ suddenly moving inward with a constant velocity $-V$, driving a shock wave into the constant density ($\rho = \rho_0$), quiescent ($u = 0$), zero pressure ($P = 0$) fluid it encapsulates (see Fig. 1). The objective of the problem is to determine both the trajectory of the converging shock wave $R_s(t)$ and the functional form of the flow field between the piston and the shock wave.

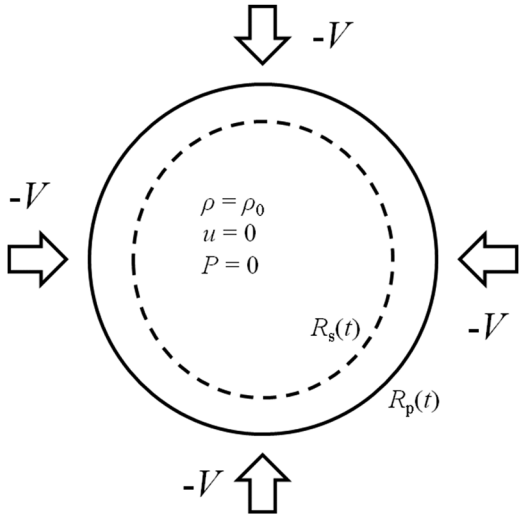

FIG. 1. The constant velocity converging curvilinear piston problem.

The 1D planar analog of this problem is fundamental in the field of gas dynamics and is discussed by Landau and Lifshitz[20] and Sachdev[25,26] among many other authors. For the case of an ideal gas EOS, the 1D planar piston problem has a closed-form solution for the shock trajectory and fluid state between the piston and shock. More broadly, the 1D planar piston problem is a member of the larger class of Riemann solutions of the 1D inviscid Euler equations, as discussed by Bethe,[31] Menikoff and Plohr,[32] and Kamm.[33] These references also include discussions surrounding the extension of the relevant Riemann solutions to flows featuring arbitrary convex EOS.

Unlike their 1D planar counterparts, 1D curvilinear piston-driven flows (be they converging or otherwise) generally have no known self-similar solutions, even for the ideal gas EOS. This phenomenon owes partially to the loss of scaling symmetries resulting from the inclusion of initial and/or boundary condition data featuring inherent dimensional scales (e.g., ρ_0 and V in the current case). Under these conditions, the remaining "universal" scaling group can only give rise to shock waves that propagate with constant velocity. However, as curvilinear shock waves typically decelerate or accelerate, the constant velocity solutions are discarded, leaving no available self-similar phenomenology. For a more detailed mathematical treatment of this topic, see the work of Boyd *et al.* and references therein.[18,27]

Accordingly, Van Dyke and Guttmann[24] treat their analysis of the ideal gas, constant velocity, converging curvilinear piston problem (henceforth referred to as the "piston problem" for brevity) in a quasisimilar fashion, employing series expansion techniques to semianalytically model the flow. The pedigree for this type of analysis was previously established by McFadden,[34] Sakurai,[35–37] Sedov,[14] and Friedman[38] (see also Sachdev[25,26]) in a variety of other (but closely related) contexts. The key feature of these analyses is the inclusion of a formally self-similar solution as the lowest-order term in the series expansion. Higher-order terms thus represent corrections to ideal self-similarity.

Published under license by AIP Publishing

An extension of Van Dyke and Guttmann's[24] work involving a nonideal material is performed by Arora and Sharma,[39] who investigate flows featuring the Van der Waals EOS. The current study features the stiff gas EOS, which is relevant to the shock compression of crystalline solids.

A. Flow equations

Consistent with previous treatments on the subject, the piston problem will be investigated in terms of the 1D inviscid compressible flow (Euler) equations

$$\frac{\partial \rho}{\partial t} + u\frac{\partial \rho}{\partial r} + \rho\left(\frac{\partial u}{\partial r} + \frac{ju}{r}\right) = 0, \tag{1}$$

$$\frac{\partial u}{\partial t} + u\frac{\partial u}{\partial r} + \frac{1}{\rho}\frac{\partial P}{\partial r} = 0, \tag{2}$$

$$\frac{\partial P}{\partial t} + u\frac{\partial P}{\partial r} + K_S\left(\frac{\partial u}{\partial r} + \frac{ju}{r}\right) = 0, \tag{3}$$

where r and t denote the independent space and time coordinates, ρ, u, and P denote the fluid mass density, radial velocity, and pressure, j is the space index ($j = 0$, 1, or 2 for 1D planar, cylindrical, or spherical symmetries), and K_S is the fluid adiabatic bulk modulus, defined by

$$K_S(\rho, P) = \rho\frac{\partial \mathscr{P}}{\partial \rho} + \frac{P}{\rho}\frac{\partial \mathscr{P}}{\partial e}, \tag{4}$$

where $P = \mathscr{P}(\rho,e)$ is the (incomplete) EOS constitutive law characterizing the material into which the piston is moving, and e is the fluid specific internal energy (energy per unit mass). Given either the adiabatic bulk modulus or EOS intrinsic properties of the material, Eqs. (1)–(3) are closed in ρ, u, and P. Equations (1)–(3) are the same as those used by Ovsiannikov[40] and Cantwell[41] in the symmetry analysis context; derivations are provided by, for example, Axford,[42] Ramsey *et al.*,[28] and Boyd *et al.*[18,27]

B. Stiff gas

A simple but useful generalization of the ideal gas EOS,

$$P = (\gamma - 1)\rho e, \tag{5}$$

is the stiff gas EOS as given by Harlow and Amsden[29]

$$P = c_0^2(\rho - \rho_0) + (\gamma - 1)\rho e, \tag{6}$$

where $\rho_0 > 0$ and $c_0 \geq 0$ are material-specific reference quantities with units of density and velocity, respectively, and $\gamma > 1$ is the material-specific (dimensionless) adiabatic index. As noted by Burnett *et al.*,[30] the stiff gas EOS may also be viewed as a linearization of the Mie-Gruneisen EOS often employed to characterize the shock compression of crystalline solids. As such, the parameters ρ_0, c_0, and γ appearing in Eq. (6) may be obtained (for example) from empirical shock velocity-particle velocity (us-up) relations of the form

$$u_s = c_0 + su_p, \tag{7}$$

where $\gamma = 2s$, and ρ_0 is the ambient density of the material in question (see, for example, Meyers[43] or Cooper[44]). Alternate u_s-u_p relations also exist and may result in alternate forms of both the Mie-Gruneisen EOS and Eq. (6). However, Eq. (6) has been found to be appropriate to model the shock compression of various metals, water, and other nonideal substances. The stiff gas EOS also allows for tension processes as well as compression.

Moreover, with Eq. (6), Eq. (4) may be used to compute the adiabatic bulk modulus for the stiff gas EOS

$$K_S = \rho_0 c_0^2 + \gamma P, \tag{8}$$

which remains nonzero even as $P \to 0$, unlike the ideal gas EOS. This behavior is characteristic of many liquid or solid materials.

Finally, with Eq. (8), Eq. (3) becomes

$$\frac{\partial P}{\partial t} + u\frac{\partial P}{\partial r} + \left(\rho_0 c_0^2 + \gamma P\right)\left(\frac{\partial u}{\partial r} + \frac{ju}{r}\right) = 0, \tag{9}$$

which, with Eqs. (1) and (2), is closed in ρ, u, and P.

C. Shock jump conditions

The inviscid Euler equations admit discontinuous solutions some of which may be interpreted as flows featuring shock waves. The inviscid Euler equations themselves do not hold at the exact position of a shock, but when cast in conservation form, they may be used to derive conservation relations connecting the flow states immediately to either side. These expressions are known as the Rankine-Hugoniot jump conditions and express conservation of mass, momentum, and total energy across the shock. They are given by (see, for example, the work of Zel'dovich and Raizer[21])

$$\left(u_2 - \dot{R}_s\right)\rho_2 = \left(u_1 - \dot{R}_s\right)\rho_1, \tag{10}$$

$$P_2 + \left(u_1 - \dot{R}_s\right)\rho_1 u_2 = P_1 + \left(u_1 - \dot{R}_s\right)\rho_1 u_1, \tag{11}$$

$$e_2 + \frac{P_2}{\rho_2} + \frac{\left(u_2 - \dot{R}_s\right)^2}{2} = e_1 + \frac{P_1}{\rho_1} + \frac{\left(u_1 - \dot{R}_s\right)^2}{2}, \tag{12}$$

where the subscripts "1" and "2" denote the unperturbed and perturbed states, respectively, and the overdot applied to the shock position R_s denotes time differentiation.

For the stiff gas EOS, Eq. (6) may be used to eliminate e from Eq. (12) to yield

$$\frac{\gamma P_2}{(\gamma-1)\rho_2} + \frac{\left(u_2 - \dot{R}_s\right)^2}{2} - \frac{c_0^2(\rho_2 - \rho_0)}{(\gamma-1)\rho_2} = \frac{\gamma P_1}{(\gamma-1)\rho_1} + \frac{\left(u_1 - \dot{R}_s\right)^2}{2} - \frac{c_0^2(\rho_1 - \rho_0)}{(\gamma-1)\rho_1}, \tag{13}$$

where it has been assumed that the unshocked density of the gas is the same as the stiff gas reference density ρ_0. Indeed, for the piston problem described in Sec. II, the unshocked state of the gas is prescribed so that $\rho_1 = \rho_0$, $u_1 = 0$, and $P_1 = 0$. With these conditions, Eqs. (10), (11), and (13) become, respectively,

$$\rho_2 = \rho_0\frac{(\gamma+1)\dot{R}_s^2}{2c_0^2 + (\gamma-1)\dot{R}_s^2}, \tag{14}$$

$$u_2 = \frac{2}{\gamma+1}\left(\dot{R}_s - \frac{c_0^2}{\dot{R}_s}\right), \tag{15}$$

$$P_2 = \frac{2}{\gamma+1}\rho_0\left(\dot{R}_s^2 - c_0^2\right), \tag{16}$$

Published under license by AIP Publishing

which is an underdetermined system for ρ_2, u_2, P_2, and $\dot{R}_s$. Equations (14)–(16) indicate $|\dot{R}_s| > c_0$ for the shock wave to be compressive (i.e., $P_2 > 0$ or $\rho_2 > \rho_0$).

In any event, Eqs. (14)–(16) are underdetermined because insufficient information has been provided for the shocked state of the gas. From the piston problem definition, the only unused condition is $u = -V$ at the position of the piston $R_p(t)$; no information is provided at the location of the shock wave, immediately adjacent to which states 1 and 2 are defined. However, in the case of 1D planar geometry ($j = 0$), curvilinear effects are absent so that

$$u = -V \quad \text{when} \quad R_s < r \le R_p, \tag{17}$$

thus implying $u_2 = -V$. In this case, the solution of Eqs. (14)–(16) for ρ_2, P_2, and $\dot{R}_s$ is given by

$$\rho_2 = \rho_0 \frac{4c_0^2 + (\gamma+1)V^2 + V\sqrt{16c_0^2 + (\gamma+1)^2V^2}}{4c_0^2 + 2(\gamma-1)V^2}, \tag{18}$$

$$P_2 = \frac{\rho_0}{4}\left[(\gamma+1)V^2 + V\sqrt{16c_0^2 + (\gamma+1)^2V^2}\right], \tag{19}$$

$$\dot{R}_s = -\frac{1}{4}\left[(\gamma+1)V + \sqrt{16c_0^2 + (\gamma+1)^2V^2}\right]. \tag{20}$$

In the ideal gas limit (i.e., $c_0 \to 0$), the positive solution branch of Eqs. (18)–(20) recovers the ideal gas planar piston result given by Van Dyke and Guttmann[24] or Landau and Lifshitz.[20]

Otherwise, Eqs. (18)–(20) are valid only for 1D planar geometry ($j = 0$). For 1D cylindrical or spherical geometry, Eq. (17) does not hold, in general, and $u = -V$ only at $r = R_p(t)$. This result is intuitive in that Eq. (20) predicts a constant shock velocity; for the case of curvilinear geometry, the shock wave is expected to accelerate toward the axis or point of symmetry, thus contradicting Eq. (20). In this scenario, Eqs. (14)–(16) must instead be used.

D. Dimensionless interpretation

As written, Eqs. (1), (2), (9), and (14)–(16) may be rendered dimensionless through a change to the dimensionless variables

$$\tilde{r} \to r/R_{p,0},$$

$$\tilde{t} \to tV/R_{P,0},$$

$$\tilde{\rho} \to \rho/\rho_0,$$

$$\tilde{u} \to u/V,$$

$$\tilde{P} \to P/\rho_0 V^2,$$

$$\tilde{c}_0 \to c_0/V,$$

$$\dot{\tilde{R}}_s \to \dot{R}_s/V,$$

under which Eqs. (1), (2), and (9) become, respectively,

$$\frac{\partial\tilde{\rho}}{\partial\tilde{t}} + \tilde{u}\frac{\partial\tilde{\rho}}{\partial\tilde{r}} + \tilde{\rho}\left(\frac{\partial\tilde{u}}{\partial\tilde{r}} + \frac{j\tilde{u}}{\tilde{r}}\right) = 0, \tag{21}$$

$$\frac{\partial\tilde{u}}{\partial\tilde{t}} + \tilde{u}\frac{\partial\tilde{u}}{\partial\tilde{r}} + \frac{1}{\tilde{\rho}}\frac{\partial\tilde{P}}{\partial\tilde{r}} = 0, \tag{22}$$

$$\frac{\partial\tilde{P}}{\partial\tilde{t}} + \tilde{u}\frac{\partial\tilde{P}}{\partial\tilde{r}} + \left(\tilde{c}_0^2 + \gamma\tilde{P}\right)\left(\frac{\partial\tilde{u}}{\partial\tilde{r}} + \frac{j\tilde{u}}{\tilde{r}}\right) = 0, \tag{23}$$

and Eqs. (14)–(16) become, respectively,

$$\tilde{\rho}_2 = \frac{(\gamma+1)\dot{\tilde{R}}_s^2}{2\tilde{c}_0^2 + (\gamma-1)\dot{\tilde{R}}_s^2}, \tag{24}$$

$$\tilde{u}_2 = \frac{2}{\gamma+1}\left(\dot{\tilde{R}}_s - \frac{\tilde{c}_0^2}{\dot{\tilde{R}}_s}\right), \tag{25}$$

$$\tilde{P}_2 = \frac{2}{\gamma+1}\left(\dot{\tilde{R}}_s^2 - \tilde{c}_0^2\right). \tag{26}$$

This change of variables follows from the invariance of the inviscid Euler equations under a three-parameter scaling group (in the current case represented by the parameters R_0, V, and ρ_0). However, unlike the cases treated by Boyd *et al.*,[27] these transformations include a rescaling by V of the material-specific parameter c_0. This nondimensionalization is an example of a dynamic similarity transformation (as opposed to an even more specific self-similarity transformation) as discussed by Sedov[14] and Zel'dovich and Raizer[21] and, in the current case, enables "material scaling" in addition to the usual geometric Euler scaling processes. This type of scaling is analogous to material surrogacy phenomena often encountered in the context of scale modeling of flow experiments. Further consequences of this interpretation will be discussed during the course of the developments to follow.

Throughout Sec. III, the tildes will be dropped from Eqs. (21)–(26), with the assumption that all variables, parameters, and quantities will be considered as dimensionless unless otherwise indicated.

III. QUASISIMILAR SOLUTION

As noted in Sec. II, the piston problem has no known self-similar solution (in curvilinear geometry). Van Dyke and Guttmann's[24] approach to solving the problem relies on a quasisimilar analysis, where the 1D planar solution [Eqs. (18)–(20) in the current case] is taken as the lowest order term in a series solution. The higher order terms in the expansion thus represent curvilinear effects.

In the dimensionless formulation, a new independent variable is given by

$$\xi = \lambda\left(\frac{1-r}{t} - 1\right). \tag{27}$$

As defined, this variable assumes the value $\xi = 0$ at the position $r = 1 - t$ of the piston [corresponding to dimensional position $R_p(t) = R_{p,0} - Vt$]. The value of the constant λ is selected so that $\xi = 1$ at the position $r = 1 - X_1 t$ of a hypothetical planar shock wave driven by the piston [with dimensional position $R_s(t) = R_{p,0} - X_1 Vt$]. With this assumption, Eq. (27) yields

$$\lambda = \frac{1}{X_1 - 1}. \tag{28}$$

Given that the piston problem configuration described in Sec. II always results in a constant-velocity shock in 1D planar geometry,

Published under license by AIP Publishing

Eq. (28) is a general result (assuming the dimensionless planar shock velocity X_1 can be computed analytically, which depends on the form of the EOS being employed).

The quasisimilar analysis then proceeds by introducing the expansions

$$R_s = 1 - \sum_{n=1}^{\infty} X_n t^n, \tag{29}$$

$$\rho = D_1 + \sum_{n=2}^{\infty} D_n(\xi) t^{n-1}, \tag{30}$$

$$u = -1 + \sum_{n=2}^{\infty} U_n(\xi) t^{n-1}, \tag{31}$$

$$P = \Pi_1 + \sum_{n=2}^{\infty} \Pi_n(\xi) t^{n-1}, \tag{32}$$

where as $t \to 0$, the solution approaches the corresponding 1D planar result; in other words, X_1, D_1, $U_1 = -1$, and Π_1 follow from a solution of the piston problem under the assumption of 1D planar geometry [i.e., as in Eqs. (17)–(20) of Sec. II C].

Furthermore, the higher order expansion functions in D, U, and Π are assumed to follow:

$$D_n(\xi) = \sum_{k=1}^{n} D_{nk} \xi^{k-1}, \tag{33}$$

$$U_n(\xi) = \sum_{k=2}^{n} U_{nk} \xi^{k-1}, \tag{34}$$

$$\Pi_n(\xi) = \sum_{k=1}^{n} \Pi_{nk} \xi^{k-1}. \tag{35}$$

Equations (30)–(32) with Eqs. (33)–(35) are then substituted into the inviscid Euler equations given by Eqs. (21)–(23), and the shock jump conditions given by Eqs. (24)–(26). To accomplish this, all derivatives appearing in Eqs. (21)–(23) must be represented in terms of the various expansion functions

$$\frac{\partial \rho}{\partial t} = \sum_{n=2}^{\infty} \left[\frac{\partial \xi}{\partial t} \frac{dD_n}{d\xi} + \frac{(n-1) D_n}{t} \right] t^{n-1}, \tag{36}$$

$$\frac{\partial \rho}{\partial r} = \sum_{n=2}^{\infty} \left[\frac{\partial \xi}{\partial r} \frac{dD_n}{d\xi} \right] t^{n-1}, \tag{37}$$

$$\frac{\partial u}{\partial t} = \sum_{n=2}^{\infty} \left[\frac{\partial \xi}{\partial t} \frac{dU_n}{d\xi} + \frac{(n-1) U_n}{t} \right] t^{n-1}, \tag{38}$$

$$\frac{\partial u}{\partial r} = \sum_{n=2}^{\infty} \left[\frac{\partial \xi}{\partial r} \frac{dU_n}{d\xi} \right] t^{n-1}, \tag{39}$$

$$\frac{\partial P}{\partial t} = \sum_{n=2}^{\infty} \left[\frac{\partial \xi}{\partial t} \frac{d\Pi_n}{d\xi} + \frac{(n-1) \Pi_n}{t} \right] t^{n-1}, \tag{40}$$

$$\frac{\partial P}{\partial r} = \sum_{n=2}^{\infty} \left[\frac{\partial \xi}{\partial r} \frac{d\Pi_n}{d\xi} \right] t^{n-1}, \tag{41}$$

$$\dot{R}_s = -\sum_{n=1}^{\infty} n X_n t^{n-1}, \tag{42}$$

where the derivatives of the quasisimilarity variable ξ are given by, with Eq. (27),

$$\frac{\partial \xi}{\partial t} = \frac{-(\xi + \lambda)}{t}, \tag{43}$$

$$\frac{\partial \xi}{\partial r} = -\frac{\lambda}{t}, \tag{44}$$

and the derivatives of the expansion functions D_n, U_n, and Π_n are, with Eqs. (33)–(35),

$$\frac{dD_n}{d\xi} = \sum_{k=1}^{n} (k-1) D_{nk} \xi^{k-2}, \tag{45}$$

$$\frac{dU_n}{d\xi} = \sum_{k=2}^{n} (k-1) U_{nk} \xi^{k-2}, \tag{46}$$

$$\frac{d\Pi_n}{d\xi} = \sum_{k=1}^{n} (k-1) \Pi_{nk} \xi^{k-2}. \tag{47}$$

With Eqs. (30)–(46), Eqs. (21)–(23) become, respectively,

$$\begin{aligned}
&[\lambda - t(\xi+\lambda)] \sum_{n=2}^{\infty} \left[-(\xi+\lambda) \sum_{k=1}^{n} (k-1) D_{nk} \xi^{k-2} + (n-1) \sum_{k=1}^{n} D_{nk} \xi^{k-1} \right] t^{n-2} - \lambda [\lambda - t(\xi+\lambda)] \left[-1 + \sum_{n=2}^{\infty} \sum_{k=2}^{n} U_{nk} \xi^{k-1} t^{n-1} \right] \\
&\quad \times \sum_{n=2}^{\infty} \sum_{k=1}^{n} (k-1) D_{nk} \xi^{k-2} t^{n-2} + \left(D_1 + \sum_{n=2}^{\infty} \sum_{k=1}^{n} D_{nk} \xi^{k-1} t^{n-1} \right) \left\{ -\lambda [\lambda - t(\xi+\lambda)] \sum_{n=2}^{\infty} \sum_{k=2}^{n} (k-1) U_{nk} \xi^{k-2} t^{n-2} \right. \\
&\quad \left. + j\lambda \left[-1 + \sum_{n=2}^{\infty} \sum_{k=2}^{n} U_{nk} \xi^{k-1} t^{n-1} \right] \right\} = 0,
\end{aligned} \tag{48}$$

$$\begin{aligned}
&\left(D_1 + \sum_{n=2}^{\infty} \sum_{k=1}^{n} D_{nk} \xi^{k-1} t^{n-1} \right) \sum_{n=2}^{\infty} \left[-(\xi+\lambda) \sum_{k=2}^{n} (k-1) U_{nk} \xi^{k-2} + (n-1) \sum_{k=2}^{n} U_{nk} \xi^{k-1} \right] t^{n-2} - \lambda \left(D_1 + \sum_{n=2}^{\infty} \sum_{k=1}^{n} D_{nk} \xi^{k-1} t^{n-1} \right) \\
&\quad \times \left[-1 + \sum_{n=2}^{\infty} \sum_{k=2}^{n} U_{nk} \xi^{k-1} t^{n-1} \right] \sum_{n=2}^{\infty} \sum_{k=2}^{n} (k-1) U_{nk} \xi^{k-2} t^{n-2} - \lambda \sum_{n=2}^{\infty} \sum_{k=1}^{n} (k-1) \Pi_{nk} \xi^{k-2} t^{n-2} = 0,
\end{aligned} \tag{49}$$

Published under license by AIP Publishing

$$[\lambda - t(\xi+\lambda)]\sum_{n=2}^{\infty}\left[-(\xi+\lambda)\sum_{k=1}^{n}(k-1)\Pi_{nk}\xi^{k-2} + (n-1)\sum_{k=1}^{n}\Pi_{nk}\xi^{k-1}\right]t^{n-2} - \lambda[\lambda - t(\xi+\lambda)]\left[-1+\sum_{n=2}^{\infty}\sum_{k=2}^{n}U_{nk}\xi^{k-1}t^{n-1}\right]$$
$$\times\sum_{n=2}^{\infty}\sum_{k=1}^{n}(k-1)\Pi_{nk}\xi^{k-2}t^{n-2} + \left[c_0^2 + \gamma\left(\Pi_1 + \sum_{n=2}^{\infty}\sum_{k=1}^{n}\Pi_{nk}\xi^{k-1}t^{n-1}\right)\right]\left\{-\lambda[\lambda - t(\xi+\lambda)]\sum_{n=2}^{\infty}\sum_{k=2}^{n}(k-1)U_{nk}\xi^{k-2}t^{n-2}\right.$$
$$\left. + j\lambda\left[-1+\sum_{n=2}^{\infty}\sum_{k=2}^{n}U_{nk}\xi^{k-1}t^{n-1}\right]\right\} = 0. \tag{50}$$

In addition to Eqs. (21)–(23), Eqs. (24)–(26) must also be similarly transformed, yielding, respectively,

$$\left(D_1 + \sum_{n=2}^{\infty}\sum_{k=1}^{n}D_{nk}\xi_s^{k-1}t^{n-1}\right)\left[2c_0^2 + (\gamma-1)\left(\sum_{n=1}^{\infty}nX_nt^{n-1}\right)^2\right]$$
$$-(\gamma+1)\left(\sum_{n=1}^{\infty}nX_nt^{n-1}\right)^2 = 0, \tag{51}$$

$$\left(-1+\sum_{n=2}^{\infty}\sum_{k=2}^{n}U_{nk}\xi_s^{k-1}t^{n-1}\right)\sum_{n=1}^{\infty}nX_nt^{n-1}$$
$$-\frac{2}{\gamma+1}\left[c_0^2 - \left(\sum_{n=1}^{\infty}nX_nt^{n-1}\right)^2\right] = 0, \tag{52}$$

$$\Pi_1 + \sum_{n=2}^{\infty}\sum_{k=1}^{n}\Pi_{nk}\xi_s^{k-1}t^{n-1} - \frac{2}{\gamma+1}\left[\left(\sum_{n=1}^{\infty}nX_nt^{n-1}\right)^2 - c_0^2\right] = 0. \tag{53}$$

As indicated, Eqs. (51)–(53) are valid only at $\xi = \xi_s$, the ξ-position of the curvilinear shock wave (and not $\xi = 1$, the position of the hypothetical planar shock wave). With Eqs. (27)–(29), this position is given by

$$\xi_s = \xi(r = R_s) = 1 + \frac{1}{X_1 - 1}\sum_{n=2}^{\infty}X_nt^{n-1}. \tag{54}$$

Equations (48)–(53) are approximately solved by collecting in powers of time and setting each coefficient of those powers to zero. For example, if each series in n appearing in the previous developments is truncated at $N = 2$, Eqs. (48)–(53) yield, respectively,

$$[\lambda - t(\xi+\lambda)](-\lambda D_{22} + D_{21}) - \lambda[\lambda - t(\xi+\lambda)](-1+U_{22}\xi t)D_{22}$$
$$+(D_1 + D_{21}t + D_{22}\xi t)\{-\lambda[\lambda - t(\xi+\lambda)]U_{22}$$
$$+j\lambda(-1+U_{22}\xi t)\} = 0, \tag{55}$$

$$-\lambda U_{22}(D_1 + D_{21}t + D_{22}\xi t) - \lambda(D_1 + D_{21}t + D_{22}\xi t)(-1+U_{22}\xi t)U_{22}$$
$$-\lambda\Pi_{22} = 0, \tag{56}$$

$$[\lambda - t(\xi+\lambda)](-\lambda\Pi_{22} + \Pi_{21}) - \lambda[\lambda - t(\xi+\lambda)](-1+U_{22}\xi t)\Pi_{22}$$
$$+\left[c_0^2 + \gamma(\Pi_1 + \Pi_{21}t + \Pi_{22}\xi t)\right]\{-\lambda[\lambda - t(\xi+\lambda)]U_{22}$$
$$+j\lambda(-1+U_{22}\xi t)\} = 0, \tag{57}$$

$$(D_1 + D_{21}t + D_{22}\xi_s t)\left[2c_0^2 + (\gamma-1)(X_1 + 2X_2t)^2\right]$$
$$-(\gamma+1)(X_1 + 2X_2t)^2 = 0, \tag{58}$$

$$(-1+U_{22}\xi_s t)(X_1 + 2X_2t) - \frac{2}{\gamma+1}\left[c_0^2 - (X_1 + 2X_2t)^2\right] = 0, \tag{59}$$

$$\Pi_1 + \Pi_{21}t + \Pi_{22}\xi_s t - \frac{2}{\gamma+1}\left[(X_1 + 2X_2t)^2 - c_0^2\right] = 0, \tag{60}$$

where, from Eq. (54),

$$\xi_s = 1 + \frac{X_2t}{X_1 - 1}. \tag{61}$$

The t^0 powers of Eqs. (55)–(60) are, respectively,

$$D_{21} - D_1(\lambda U_{22} + j) = 0, \tag{62}$$

$$\lambda\Pi_{22} = 0, \tag{63}$$

$$\Pi_{21} - \left(c_0^2 + \gamma\Pi_1\right)(\lambda U_{22} + j) = 0, \tag{64}$$

$$D_1\left[2c_0^2 + (\gamma-1)X_1^2\right] - (\gamma+1)X_1^2 = 0, \tag{65}$$

$$X_1 + \frac{2}{\gamma+1}\left(c_0^2 - X_1^2\right) = 0, \tag{66}$$

$$\Pi_1 - \frac{2}{\gamma+1}\left(X_1^2 - c_0^2\right) = 0. \tag{67}$$

Equations (65)–(67) may be solved independently of Eqs. (62)–(64) to yield the dimensionless form of Eqs. (18)–(20)

$$D_1 = \frac{4c_0^2 + (\gamma+1) + \sqrt{16c_0^2 + (\gamma+1)^2}}{4c_0^2 + 2(\gamma-1)}, \tag{68}$$

$$\Pi_1 = \frac{1}{4}\left[(\gamma+1) + \sqrt{16c_0^2 + (\gamma+1)^2}\right], \tag{69}$$

$$X_1 = \frac{1}{4}\left[(\gamma+1) + \sqrt{16c_0^2 + (\gamma+1)^2}\right]. \tag{70}$$

However, even with these expressions, Eqs. (62)–(64) are not a closed system for D_{21}, U_{22}, Π_{21}, and Π_{22}. This system is closed by adding the t^1 powers of Eqs. (58)–(60)

$$4(\gamma-1)(D_1 - 1)X_1X_2 + (D_{21} + D_{22})\left[2c_0^2 + (\gamma-1)X_1^2\right] = 0, \tag{71}$$

Published under license by AIP Publishing

$$-2X_2 + U_{22}X_1 + \frac{8}{\gamma+1}X_1X_2 = 0, \tag{72}$$

$$\Pi_{21} + \Pi_{22} - \frac{8}{\gamma+1}X_1X_2 = 0. \tag{73}$$

Equations (62)–(64) and (71)–(73) are a closed system for D_{21}, D_{22}, U_{22}, Π_{21}, Π_{22}, and X_2, the solution of which is given by

$$D_{21} = \frac{4jD_1X_1^2}{4X_1^2 + \lambda[4X_1 - (\gamma+1)]\left(c_0^2 + \gamma\Pi_1\right)}, \tag{74}$$

$$D_{22} = -\frac{2jX_1^2\left\{c_0^2\left[\left(3+\gamma^2\right)D_1 - (\gamma+1)^2\right] + \gamma(\gamma+1)[(\gamma-1)D_1 - (\gamma+1)]\Pi_1 + 2(\gamma-1)D_1X_1^2\right\}}{\left[2c_0^2 + (\gamma-1)X_1^2\right]\left\{4X_1^2 + \lambda[4X_1 - (\gamma+1)]\left(c_0^2 + \gamma\Pi_1\right)\right\}}, \tag{75}$$

$$U_{22} = \frac{j\left(c_0^2 + \gamma\Pi_1\right)[(\gamma+1) - 4X_1]}{4X_1^2 + \lambda[4X_1 - (\gamma+1)]\left(c_0^2 + \gamma\Pi_1\right)}, \tag{76}$$

$$\Pi_{21} = \frac{4jX_1^2\left(c_0^2 + \gamma\Pi_1\right)}{4X_1^2 + \lambda[4X_1 - (\gamma+1)]\left(c_0^2 + \gamma\Pi_1\right)}, \tag{77}$$

$$\Pi_{22} = 0, \tag{78}$$

$$X_2 = \frac{j(\gamma+1)X_1\left(c_0^2 + \gamma\Pi_1\right)}{2\left\{4X_1^2 + \lambda[4X_1 - (\gamma+1)]\left(c_0^2 + \gamma\Pi_1\right)\right\}}. \tag{79}$$

With Eqs. (68)–(70) for D_1, Π_1, and X_1 and Eq. (28) for λ, Eqs. (74)–(79) fully determine the $n = 2$ correction to the 1D planar piston problem as given in Eqs. (29)–(32). In the limit $c_0 \to 0$, Eqs. (68)–(70) and (28) become, respectively,

$$D_1 = \frac{\gamma+1}{\gamma-1}, \tag{80}$$

$$\Pi_1 = \frac{\gamma+1}{2}, \tag{81}$$

$$X_1 = \frac{\gamma+1}{2}, \tag{82}$$

$$\lambda = \frac{2}{\gamma-1}, \tag{83}$$

and Eqs. (74)–(79) collapse to

$$D_{21} = \frac{j(\gamma+1)}{2\gamma-1}, \tag{84}$$

$$D_{22} = -\frac{j(\gamma+1)}{2\gamma-1}, \tag{85}$$

$$U_{22} = -\frac{j\gamma(\gamma-1)}{2(2\gamma-1)}, \tag{86}$$

$$\Pi_{21} = \frac{j\gamma(\gamma+1)(\gamma-1)}{2(2\gamma-1)}, \tag{87}$$

$$\Pi_{22} = 0, \tag{88}$$

$$X_2 = \frac{j\gamma(\gamma+1)(\gamma-1)}{8(2\gamma-1)}, \tag{89}$$

which is identical to the result for an ideal gas given by Van Dyke and Guttmann.[24]

Following this procedure for arbitrary N, the quasisimilar analysis results in a system of $3N$ algebraic equations for the expansion coefficients D_{nk}, U_{nk}, Π_{nk}, and X_n. Each such system depends on all lower order approximations (e.g., the D_3, U_3, Π_3, and X_3 coefficients depend on the D_1, D_2, U_1, U_2, Π_1, Π_2, X_1, and X_2 coefficients); although as was the case for $N = 2$, these systems may be solved sequentially. While the results of this exercise rapidly become algebraically cumbersome for $N > 2$, they are easily obtained via a symbolic algebra package.

A. Numerical example for copper

The quasisimilar procedure illustrated in Sec. III may be numerically evaluated to high order when the various material, geometry, and expansion parameters prescribed therein are specified. As an example, copper (Cu) is well-characterized by linear u_s-u_p data of the form given by Eq. (7); these data may in turn be used to infer a stiff gas EOS. The parameterization for Cu given by Cooper[44] is

$$\rho_0 = 8.930\ \text{g/cm}^3,$$

$$c_0 = 3.940\ \text{km/s},$$

$$s = \gamma/2 = 1.489.$$

Moreover, it will be further assumed that

$$j = 2,$$

$$N = 6,$$

corresponding to 1D spherical symmetry and six quasisimilar expansion terms, respectively.

Furthermore, as noted in Sec. II D, all developments and results appearing in Sec. III are dimensionless. In addition to the unshocked density ρ_0, the initial piston radius $R_{p,0}$ and piston velocity V must also be prescribed to enable conversion back to physical variables. However, while ρ_0 and $R_{p,0}$ appear in Sec. II D only as renormalization constants in converting between dimensionless and dimensional variables, V appears more directly throughout the results appearing in Sec. III as

$$\tilde{c}_0 = \frac{c_0}{V}. \tag{90}$$

Published under license by AIP Publishing

Much like the adiabatic index γ, this parameter appears explicitly in Eqs. (74)–(79) (for example). This phenomenon indicates that while the dimensionless results of the quasisimilar analysis may ostensibly be evaluated for any $\tilde{c}_0$, Eq. (90) must hold in the subsequent transformation back to physical variables. Accordingly,

- If $\tilde{c}_0$ and c_0 are specified, Eqs. (74)–(79) are only valid for one value of V.
- If $\tilde{c}_0$ and V are specified, Eqs. (74)–(79) are only valid for one value of c_0.

Similar behavior appears in previous work featuring the ideal gas EOS [e.g., Eqs. (84)–(89)], in which the resulting equations must be repeatedly evaluated for each value of γ (i.e., there is no scaling with respect to this parameter). In Sec. III, the additional parameter c_0 behaves in same way. As such, when c_0 assumes a nonzero value, V is removed from the list of scaling parameters that may assume any value (i.e., leaving only ρ_0 and $R_{p,0}$), and instead must satisfy Eq. (90). This outcome is a direct result of the presence of the intrinsic dimensional constant c_0 appearing in the stiff gas EOS; the presence of this constant reduces the rank of the admitted scaling group corresponding to Eqs. (1)–(3), as discussed in detail by Ovsiannikov,[40] Ramsey and Baty,[45] and Boyd *et al.*[18,27]

Despite these notions, Eq. (90) enables "material scaling" processes. For example, the quasisimilar analysis outlined in Sec. III may be numerically evaluated for any choice of γ, $\tilde{c}_0$, and j. In the subsequent transformation back to physical variables, Eq. (90) must be enforced. This constraint does not require a unique (c_0, V) pair in that it may be satisfied for any pair (ac_0, aV), where a is an arbitrary constant. As a result, any scaling in the piston velocity V must be accompanied by an identical scaling in c_0 (but not γ), thus selecting a new or modified material.

In any event, for the purposes of the numerical example,

$$\tilde{c}_0 = 1.0,$$

thus enabling either a quasisimilar solution for the single value of $V = 3.940$ km/s if the value $c_0 = 3.940$ km/s for Cu is employed or a family of solutions satisfying Eq. (90) if no data for either c_0 or V is prescribed. The results of these calculations for the converging shock wave trajectory are provided in Table I; with these results, the trajectory may be reconstructed using Eq. (29).

Figure 2 depicts both the piston trajectory and the $N = 1$ and $N = 6$ converging shock wave trajectories reconstructed using Table I. Figure 2 shows that high-order terms are most influential near times, where the converging shock wave reaches $r = 0$, and allow for the shock to accelerate (as is typical of converging shock waves in curvilinear geometries and demonstrated by the nontrivial curvature

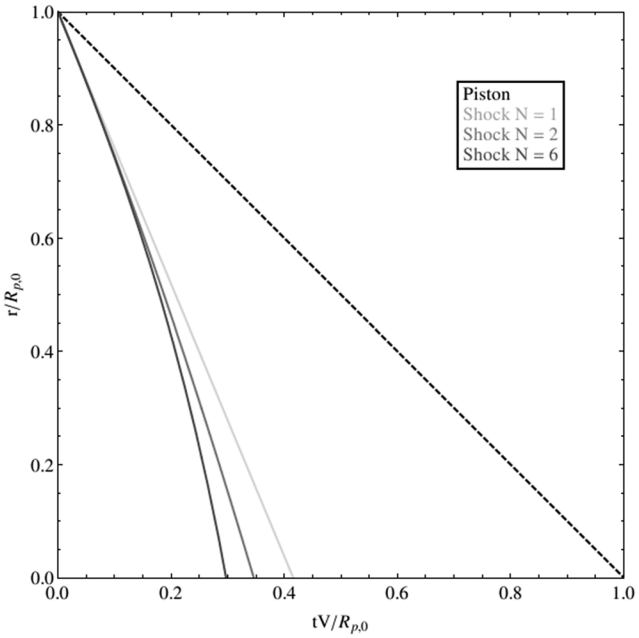

FIG. 2. Piston trajectory and converging shock wave trajectory estimates for Cu example.

of the $N = 2$ and $N = 6$ trajectories appearing in Fig. 2). The time t_c at which the shock converges to $r = 0$ can be estimated from a root extraction of Eq. (29) and is also provided in Table I. Following Van Dyke and Guttmann[24] (see also Sachdev[25,26]), and under Guderley's[1] assumption that the shock trajectory has the $t \to t_c$ limit given by

$$R_s \to R_{p,0}\left(1 - \frac{t}{t_c}\right)^{\alpha}, \tag{91}$$

the constant α may be estimated as

$$\alpha \sim \left(1 - \frac{X_n}{X_{n-1}} t_c\right) n - 1, \tag{92}$$

and constructed from the X_n and t_c information appearing in Table I. These values of α are interpreted as increasingly accurate (with increasing n) approximations to the Guderley similarity exponent appearing in the works of Guderley,[1] Lazarus,[4] and Ramsey *et al.*[11] among many others. However, in this case, the similarity exponent corresponds to a converging shock wave in a stiff gas, as opposed to an ideal gas. These results thus correspond to the

TABLE I. X_n values for Cu example.

n	X_n	t_c from Eq. (29)	α from Eq. (92)
1	2.405	0.4158	...
2	1.397	0.3462	0.5978
3	2.461	0.3217	0.2998
4	5.318	0.3095	0.3248
5	13.02	0.3023	0.2994
6	34.50	0.2975	0.2702

TABLE II. D_{nk} values for Cu example.

	$k = 1$	$k = 2$	$k = 3$	$k = 4$	$k = 5$	$k = 6$
$n = 2$	1.417	−0.8249	...	...	...	...
$n = 3$	3.427	0.2845	−2.154	...	...	...
$n = 4$	7.073	−1.962	11.11	−9.687	...	...
$n = 5$	14.05	−3.179	5.021	35.51	−28.30	...
$n = 6$	28.13	−7.256	29.35	−51.25	163.8	−94.77

Published under license by AIP Publishing

TABLE III. U_{nk} values for Cu example.

	$k=1$	$k=2$	$k=3$	$k=4$	$k=5$	$k=6$
$n=2$	0.0	1.6471	...	...	...	...
$n=3$	0.0	−1.853	4.287	...	...	...
$n=4$	0.0	−8.417	3.657	6.573	...	...
$n=5$	0.0	−19.88	−6.194	5.567	14.10	...
$n=6$	0.0	−42.56	−32.15	−5.480	4.390	32.19

TABLE IV. Π_{nk} values for Cu example.

	$k=1$	$k=2$	$k=3$	$k=4$	$k=5$	$k=6$
$n=2$	6.754	0.0	...	...	...	...
$n=3$	21.87	0.0	−0.094	...	...	...
$n=4$	61.96	0.0	25.39	−14.99	...	...
$n=5$	165.4	0.0	113.4	−7.401	−32.13	...
$n=6$	425.8	0.0	361.2	122.2	−69.20	−64.06

limiting behavior of a converging shock wave problem that does not otherwise have a self-similar representation (for reasons set forth by Ramsey and Baty,[45] Ramsey *et al.*,[28] and Boyd *et al.*[18,27]).

The sequence of approximate α calculations shown in Table I is also connected to the convergence behavior of the quasisimilar solution. Equation (92) itself—arising from Van Dyke and Guttmann's original implementation of the Domb and Sykes method[24]—is akin to the well-known ratio test for determining the convergence properties of a series; that $\alpha < 1$ for all values of N considered lends credence to the notion that the quasisimilar approximation is convergent for $t \leq t_c$. For the case of an ideal gas, Van Dyke and Guttmann[24] further verified this behavior up to $N = 40$; while the results for a stiff gas are expected to behave similarly to high order, for the purposes of this work, the results appearing in Table I are sufficient to demonstrate that this trend is likely to hold.

In addition to the converging shock wave trajectory, the quasisimilar methodology also provides approximate state variable profiles as functions of space and time. The coefficients D_{nk}, U_{nk}, and Π_{nk} needed to construct these profiles via Eqs. (30)–(35) are

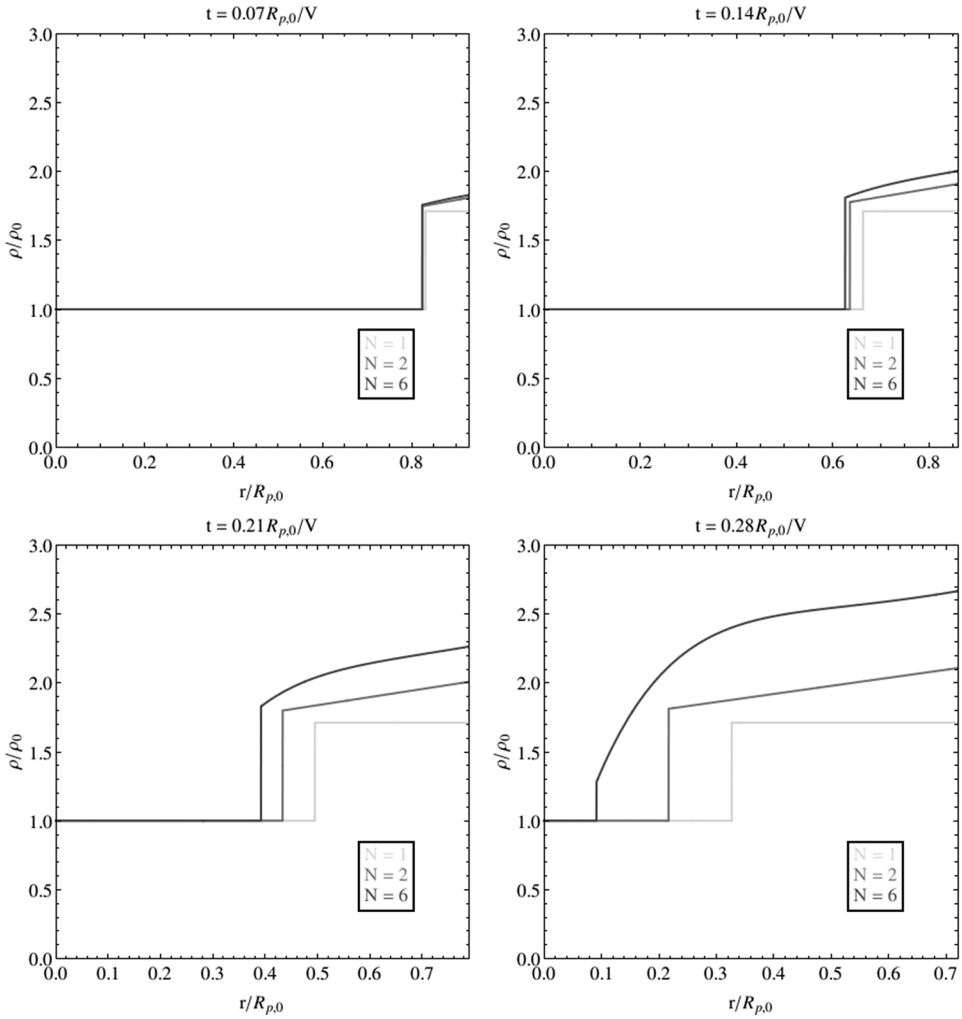

FIG. 3. Density profiles at various times for Cu example. In each plot, the rightmost limit in r represents the location of the piston at the indicated time.

Published under license by AIP Publishing

provided in Tables II–IV. Using these results, spatial density, velocity, and pressure profiles at various times are provided for $N = 1$, $N = 2$, and $N = 6$ in Figs. 3–5.

Figures 3–5 show that the $N = 1$ solution to the piston problem does not vary with r, consistent with the interpretation of this solution as corresponding the 1D planar piston problem. Curvilinear effects appear in all flow variables beginning with the $N = 2$ solution; in the case of density and velocity, the $N = 2$ solution features linear curvature in r, while the pressure solution remains spatially constant but enhanced in magnitude with respect to its $N = 1$ value. The $N = 6$ solution manifests significant nonlinear curvature in all flow variables, which otherwise begin to assume some canonical features associated with the Guderley converging shock solution (see, for example, the work of Stanyukovich,[2] Zel'dovich and Raizer,[21] or Ramsey *et al.*[11]):

- The density increases with increasing r for all times,
- The pressure features a maximum in $r > R_s(t)$,
- The velocity and pressure at $r = R_s(t)$ increase without limit as $t \to t_c$.

These features become more pronounced as $t \to t_c$ and are consistent with Guderley's[1] limiting assumption as given by Eq. (91). However, unlike the classical Guderley solution, the $N = 6$ solution depicted in Figs. 3–5 features some non-self-similar phenomena. For example, the velocity field always obeys $u(r = R_p(t)) = -V$, as expected from the definition of the piston problem given in Sec. II.

Consistent with Fig. 2, Figs. 3–5 show that for a given time, the computed shock location moves closer to $r = 0$ with increasing N. Also consistent with this phenomenon, for a given time, the computed densities, velocities, and pressures are all larger with increasing N. This behavior results from the higher-order expansions in N capturing the acceleration of the converging shock wave with increasing precision.

Moreover, Fig. 3 shows that the shock density ratio (i.e., the value of ρ/ρ_0 at the position of the shock) is not constant through time. While Eq. (24) indicates that this behavior is expected for the stiff gas EOS, it also indicates that the shock density ratio should approach a constant value as the shock wave approaches the origin

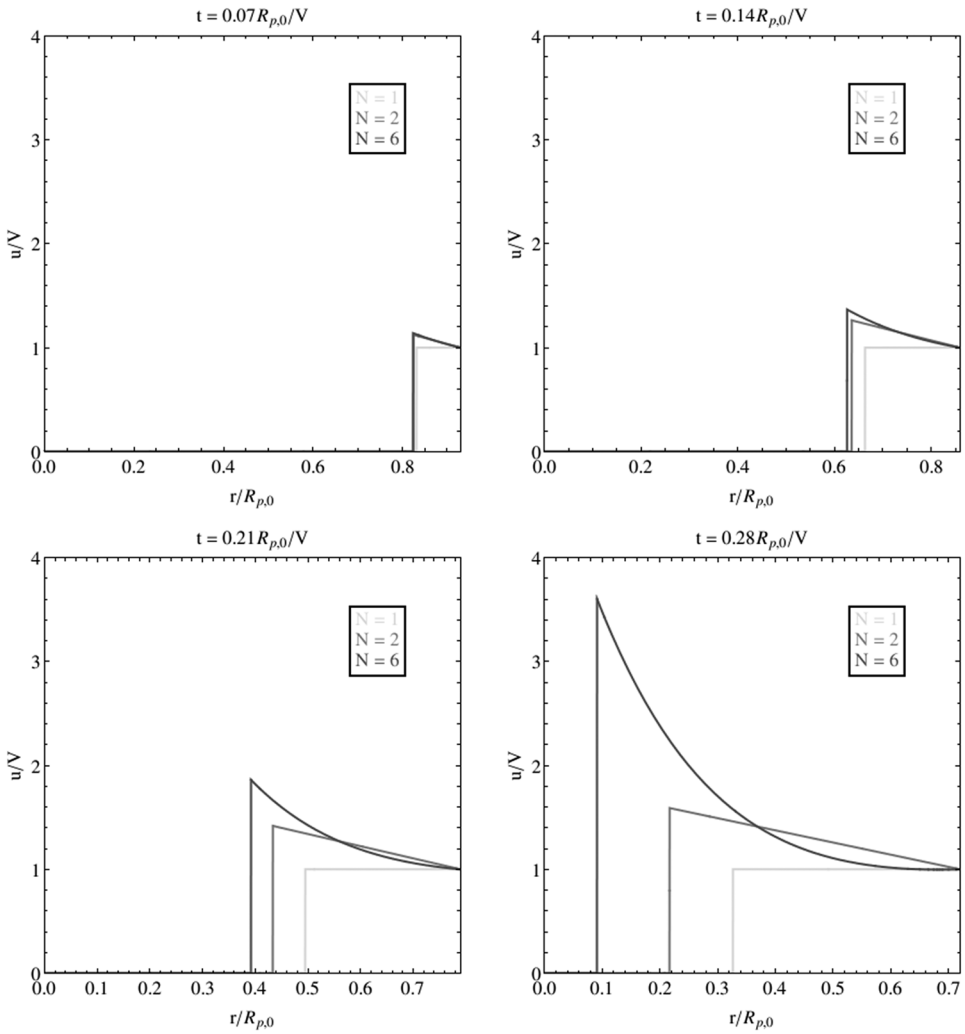

FIG. 4. Velocity profiles at various times for Cu example. In each plot, the rightmost limit in r represents the location of the piston at the indicated time.

Published under license by AIP Publishing

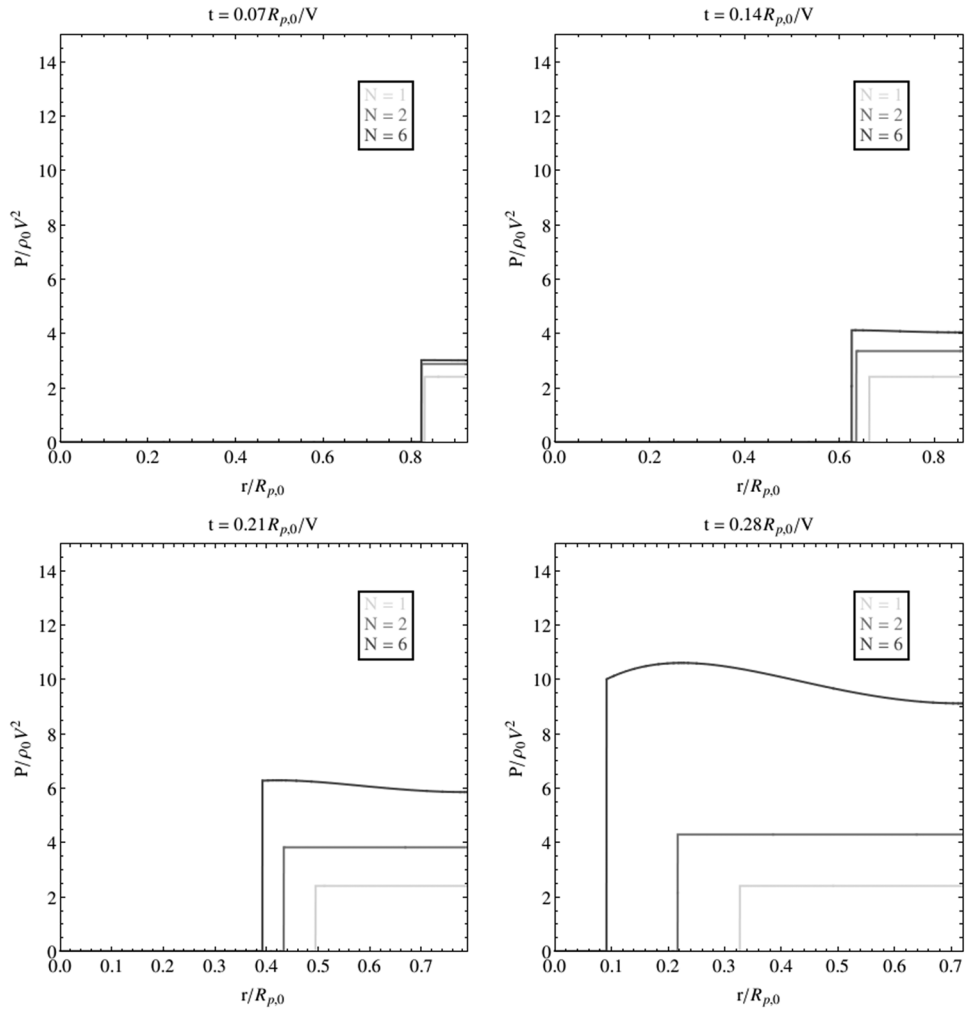

FIG. 5. Pressure profiles at various times for Cu example. In each plot, the rightmost limit in r represents the location of the piston at the indicated time.

(and begins to accelerate without limit). The $t = 0.28R_{p,0}/V$ member of Fig. 3 does not reflect this phenomenology, which is indicative of the limitations of even the $N = 6$ quasisimilar solution at relatively late times. This feature is also exhibited in the $c_0 = 0$ limit and thus manifests in the ideal gas solution (as disseminated by Van Dyke and Guttmann[24]).

Indeed, either quasisimilar solution truncated at any finite order N is only an approximation to the true solution extended to infinite terms. The behavior of the shock density ratio represents one possible metric through which the accuracy of any given approximate solution may be assessed; in the current example, the $N = 6$ solution has clearly lost physical fidelity between $t = 0.21R_{p,0}/V$ and $t = 0.28R_{p,0}/V$. For any desired accuracy and a given approximate solution, an evaluation of Eq. (24) can be compared to its expected behavior on physical grounds to establish limits on the validity of the approximate solution. Other metrics may also exist for accomplishing this goal, such as evaluation of Eqs. (25) and (26), or a calculation of the shock velocity itself. In any event, it is perhaps intuitively obvious that an increasing number of quasisimilar terms are necessary to accurately capture the behavior of the flow in increasing proximity to the origin; the above methodologies reflect one possible set for quantifying this necessity for any given scenario.

IV. CONCLUSIONS

This work has explored the extension beyond the ideal gas constitutive law of Van Dyke and Guttmann's[24] quasisimilar analysis for piston driven, curvilinear, converging shock waves. Of particular interest in this work is the stiff gas EOS, which is itself a linearization of the Mie-Gruneisen EOS that is suitable for characterizing the material response of shock compressed crystalline solids. When coupled to flows in 1D curvilinear geometries, even the relatively simple stiff gas EOS does not admit a full self-similar solution associated with a converging shock wave.

In this case, the converging shock trajectory and all state variables may instead be expanded in power series so as to enable a quasisimilar solution. The solution to the associated 1D planar piston problem is taken as the lowest-order expansion term in its quasisimilar counterpart, where curvilinear effects are captured by the inclusion of all higher-order terms. In the case of the stiff gas EOS,

Published under license by AIP Publishing

the nonideal EOS effects are represented in all orders of the series expansion methodology.

The solution resulting from this procedure is algebraically cumbersome for more than two expansion terms but otherwise easily constructed using a symbolic algebra package. Given that the ideal and stiff gas EOS classes are directly relatable to one another via Eqs. (5) and (6), an important property of the solutions derived herein are their limits as $c_0 \to 0$. When this condition is met, the results of Secs. III and IV collapse to the existing results previously disseminated by Van Dyke and Guttmann.[24]

The quasisimilar equations studied in this work are dimensionless, and their numerical solution highlights an important aspect of coupling to a nonideal EOS. Unlike Van Dyke and Guttmann's[24] study featuring the ideal gas EOS, the quasisimilar solutions constructed in this work are not invariant with respect the constant piston velocity V. Instead, due to the presence of the stiffening term in the stiff gas EOS, the quantity c_0/V appears throughout the resulting quasisimilar equations. As is more typically seen to be the case with the dimensionless adiabatic index γ, the quasisimilar equations must therefore be repeatedly solved for each value of c_0/V appearing therein. When a material-specific value c_0 is also specified, the resulting solution is valid for only one value of the piston velocity V. However, when the ratio c_0/V is specified—but not c_0 or V individually—the obtained quasisimilar solution may be scaled across families of materials and piston velocities.

Otherwise, the quasisimilar solutions derived in this work bear in certain respects close resemblance to the classical Guderley converging shock solution. While quasisimilar solutions are by definition *not* self-similar, many qualitative features of closely associated self-similar flows may be contained within them, as depicted in Figs. 2–5. In this work, it has been found that these features become more pronounced as the number of expansion terms is increased and as the converging shock wave approaches the 1D curvilinear origin. While this limit is decidedly non-self-similar, Guderley's[1] original approximation as given by Eq. (91) appears to capture many of the gross features of the flow near convergence time.

A. Recommendations for future work

The preceding work may be extended in a variety of ways. Perhaps the most obvious is to move beyond the stiff gas EOS to closure models with increasing realism. The Mie-Gruneisen EOS as discussed by Harlow and Amsden[29] and Ramsey *et al.*[28] is perhaps the most logical starting choice, but others could be dictated by the desired applications of the corresponding results. In any event, given that the quasisimilar methods employed in this work require that the shock trajectory and all state variables be expressible in terms of power series, it is likely that any future developments along these lines will be confined to EOS classes that vary smoothly as functions of their arguments. Even so, the examination in this context of more theoretically exotic (but physically relevant) nonconvex or discontinuous EOS surfaces remains an additional avenue for future study.

Moreover, the preceding work focuses exclusively on constant velocity piston motions. The quasisimilar formalism should be extensible to piston motions that vary through time in a more complicated manner. Some work along these lines has been conducted for 1D planar piston problems: as noted by Sachdev,[26] Nakamura[46] investigated quadratic-in-time piston motion, while Kozmanov[47] assumed an even more general form. However, when moving to 1D curvilinear geometries, piston motions expressible in terms of a power series in time may prove most easily amenable to quasi-similar analysis in the style of this work.

The combination of these two extensions will ultimately represent a significant generalization of this and previous work. The use of a generalized EOS in conjunction with a generalized piston motion will likely represent the limit of quasisimilar analysis in this context but has the potential to be greatly relevant to and informative of not only large-scale numerical simulations of implosion processes but also physical or experimental scenarios interrogated by the same underlying physics as employed in the theoretical analysis.

ACKNOWLEDGMENTS

This work was managed by Triad National Security, LLC for the U.S. Department of Energy's NNSA, at Los Alamos National Laboratory under Contract No. 89233218CNA000001. The authors thank E. J. Albright, J. McHardy, and J. Schmidt for valuable insights into these topics.

REFERENCES

[1] K. G. Guderley, "Starke kugelige und zylinrische verdichtungsstosse in der nahe des kugelmitterpunktes bzw. Der zylinderachse," Luftfahrtforschung **19**, 302 (1942).
[2] K. Stanyukovich, *Unsteady Motion of Continuous Media* (Elsevier, 2016).
[3] D. Butler, "Converging spherical and cylindrical shocks," Armament Res. Estab. Rep. **54**, 54 (1954).
[4] R. Lazarus, "Self-similar solutions for converging shocks and collapsing cavities," SIAM J. Numer. Anal. **18**(2), 316 (1981).
[5] R. Chisnell, "An analytic description of converging shock waves," J. Fluid Mech. **354**, 357 (1998).
[6] H. Motz, *The Physics of Laser Fusion* (Academic Press, London, 1979).
[7] S. Atzeni and J. Meyer-ter-Vehn, *The Physics of Inertial Fusion: Beam Plasma Interaction, Hydrodynamics, Hot Dense Matter* (Oxford University Press, 2004).
[8] D. Clark and M. Tabak, "A self-similar isochoric implosion for fast ignition," Nucl. Fusion **47**(9), 1147 (2007).
[9] J. Rygg, "Shock convergence and mix dynamics in inertial confinement fusion," Ph.D. dissertation (Massachusetts Institute of Technology, 2006).
[10] M. Fink, W. Hillebrandt, and F. Ropke, "Double-detonation supernovae of sub-Chandrasekhar mass white dwarfs," Astron. Astrophys. **476**(3), 1133 (2007).
[11] S. Ramsey, J. Kamm, and J. Bolstad, "The Guderley problem revisited," Int. J. Comput. Fluid Dyn. **26**(2), 79 (2012).
[12] W. Noh, "Errors for calculations of strong shocks using an artificial viscosity and an artificial heat flux," J. Comput. Phys. **72**(1), 78 (1987).
[13] G. Taylor, "The formation of a blast wave by a very intense explosion I. Theoretical discussion," Proc. R. Soc. London **201**, 159 (1950).
[14] L. Sedov, *Similarity and Dimensional Methods in Mechanics* (CRC Press, 1993).
[15] G. Barenblatt, *Scaling, Self-Similarity, and Intermediate Asymptotics: Dimensional Analysis and Intermediate Asymptotics* (Cambridge University Press, 1996).
[16] G. Barenblatt, *Scaling* (Cambridge University Press, 2003).
[17] E. Waxman and D. Shvarts, "Second-type self-similar solutions to the strong explosion problem," Phys. Fluids A **5**(4), 1035 (1993).
[18] Z. Boyd, E. Schmidt, S. Ramsey, and R. Baty, "Collapsing cavities and focusing shocks in non-ideal materials," Report No. LA-UR-17-31273, Los Alamos National Laboratory, 2017.
[19] J. Kamm, "Enhanced verification test suite for physics simulation codes," Report No. SAND 2008-7813, Sandia National Laboratory, 2008.

Published under license by AIP Publishing

[20]L. Landau and E. Lifshitz, *Fluid Mechanics* (Pergamon Press, 1987).
[21]Y. Zel'dovich and Y. Raizer, *Physics of Shock Waves and High-Temperature Hydrodynamic Phenomena* (Courier Corporation, 2002).
[22]H. Hornung, D. Pullin, and N. Ponchaut, "On the question of universality of imploding shock waves," Acta Mech. **201**(1-4), 31 (2008).
[23]S. Ramsey and J. Lilieholm, "Verification assessment of piston boundary conditions for Lagragian simulation of the Guderley problem," J. Verif. Validation, Uncertainty Quantif. **2**(3), 031001 (2017).
[24]M. Van Dyke and A. Guttmann, "The converging shock wave from a spherical or cylindrical piston," J. Fluid Mech. **120**, 451 (1982).
[25]P. Sachdev, *Shock Waves and Explosions* (Chapman & Hall/CRC, Boca Raton, FL, 2004).
[26]P. Sachdev, *Self-Similarity and Beyond: Exact Solutions of Nonlinear Problems* (Chapman & Hall/CRC, Boca Raton, FL, 2000).
[27]Z. Boyd, S. Ramsey, and R. Baty, "On the existence of self-similar converging shocks in non-ideal materials," Q. J. Mech. Appl. Math. **70**(4), 401 (2017).
[28]S. Ramsey, E. Schmidt, Z. Boyd, J. Lilieholm, and R. Baty, "Converging shock flows for a Mie-Gruneisen equation of state," Phys. Fluids **30**, 046101 (2018).
[29]F. Harlow and A. Amsden, "Fluid dynamics: A LASL monograph," Report No. LA-4700, Los Alamos National Laboratory, 1971.
[30]S. Burnett, K. Honnell, S. Ramsey, and R. Singleton, "Verification studies for the Noh problem using non-ideal equations of state and finite strength shocks," J. Verif. Validation Uncertainty Quantif. **3**(2) 021002 (2018).
[31]H. Bethe, "Clearinghouse for federal scientific and technical information," Report No. PB-32189, US Department of Commerce, Washington, DC, 1942.
[32]R. Menikoff and B. Plohr, "The Riemann problem for fluid flow of real materials," Rev. Mod. Phys. **61**(1), 75 (1989).
[33]J. Kamm, "An exact, compressible one-dimensional Riemann solver for general, convex equations of state," Report No. LA-UR-15-21616, Los Alamos National Laboratory, 2015.
[34]J. McFadden, "Initial behavior of a spherical blast," J. Appl. Phys. **23**, 1269 (1952).
[35]A. Sakurai, "Blast wave theory," Technical Report No. MRC-TSR-497, Wisconsin Univ-Madison Mathematics Research Center, Madison, WI, 1964.
[36]A. Sakurai, "On the propagation and structure of the blast wave. I," J. Phys. Soc. Jpn. **8**(5), 662 (1953).
[37]A. Sakurai, "On the propagation and structure of the blast wave. II," J. Phys. Soc. Jpn. **9**(2), 256 (1954).
[38]M. Friedman, "A simplified analysis of spherical and cylindrical blast waves," J. Fluid Mech. **11**(1), 1 (1961).
[39]R. Arora and V. Sharma, "Convergence of strong shock in a Van der Waals gas," SIAM J. Appl. Math. **66**(5), 1825 (2006).
[40]L. Ovsiannikov, *Group Analysis of Differential Equations* (Academic Press, 2004).
[41]B. Cantwell, *Introduction to Symmetry Analysis* (Cambridge University Press, 2002).
[42]R. Axford, "Solutions of the Noh problem for various equations of state using Lie groups," Laser Part. Beams **18**(1), 93 (2000).
[43]M. Meyers, *Dynamic Behavior of Materials* (John Wiley & Sons, 1994).
[44]P. Cooper, *Explosives Engineering* (VCH Publishing, 1996).
[45]S. Ramsey and R. Baty, "Symmetries of the gas dynamics equations using the differential form method," J. Math. Phys. **58**(11), 111506 (2017).
[46]Y. Nakamura, "Analysis of self-similar problems of imploding shock waves by the method of characteristics," Phys. Fluids **26**, 1234 (1983).
[47]M. Kozmanov, "On the motion of piston in a polytropic gas," J. Appl. Math. Mech. **41**, 1152 (1977).

Published under license by AIP Publishing